



Adjustments for improved upper arm adjustment factor in REBA and RULA methods based on postural sway analysis

Jiale Zhu¹, Xinming Li¹

¹ Department of Mechanical Engineering, University of Alberta, Canada

ABSTRACT: Ergonomic risk assessment methods are widely utilized in the construction sector to mitigate work-related musculoskeletal disorders (WMSDs). However, current methods, such as the Rapid Entire Body Assessment (REBA) and the Rapid Upper Limb Assessment (RULA), often encounter issues related to overestimation and fluctuation, primarily due to sharp boundaries defined by ambiguous terms. Specifically, a 0° threshold is frequently used as a strict boundary for adjustment factors, disregarding minor joint movements and muscle activation. This study aims to quantify the upper arm-related risk adjustment factors in REBA and RULA by analyzing angle tolerances through muscle activation data. Angle tolerances are derived using surface electromyography (sEMG) data from specific muscles during arm abduction movement. A total of 23 participants' data are used for this study. The main results include 1) revealing 0° threshold is unsuitable as an adjustment boundary through muscle activation analysis before arm abduction. 2) identifying joint tolerance defined by the endurance limit of 10% maximal voluntary isometric contraction (%MVC). Finally, these tolerances are subsequently used to refine posture categorization within the risk rating adjustment process, resulting in a modified upper arm adjustment factor in the REBA and RULA frameworks, which incorporates posture sway for more accurate risk estimation. The outcomes of this study are expected to mitigate the overestimation and fluctuation issues inherent in REBA and RULA while introducing a novel integration of muscle status and risk detection for risk assessment.

1. INTRODUCTION

Despite advancements in automation through Industry 4.0, the physically demanding nature of construction work and its dynamic task requirements continue to make it a high-risk environment. Consequently, workers face an increased likelihood of developing work-related musculoskeletal disorders (WMSDs) [1]. In Canada alone, 18,131 work-related injuries were documented in 2022, marking a 10.9% increase from the previous year [2]. Beyond posing direct risks to worker health and safety, WMSDs contribute to higher absenteeism rates and impose substantial financial burdens on the construction industry [3]. Therefore, to foster a safer and more sustainable work environment, it is imperative to accurately assess and mitigate ergonomic risks associated with construction tasks.

Several ergonomic risk assessment methods have been developed to address the risk factors associated with WMSDs. The most widely utilized approaches include the Ovako Working Posture Analysis System (OWAS) [4], Rapid Upper Limb Assessment (RULA) [5], and Rapid Entire Body Assessment (REBA) [6]. While these methods provide systematic frameworks for risk identification, their reliance on rule-based evaluations conducted through expert observations introduces limitations regarding both cost-effectiveness and accuracy [7-9].

48 To enhance the accuracy and effectiveness of ergonomic assessment methods, advanced technologies
49 like motion capture (MoCap) system have been introduced to provide more precise posture data [10,11].
50 Moreover, IMU sensors, known for their lightweight and portable design, can be seamlessly integrated into
51 construction clothing and have demonstrated high accuracy and repeatability in field conditions [12,13].
52 Beyond joint angle analysis, surface electromyography (sEMG) [14,15] enables a more comprehensive
53 biomechanics-level analysis by detecting muscle electrical activity.
54

55 However, the effectiveness of risk evaluation is still constrained by inherent limitations in widely used
56 assessment methods such as REBA and RULA [16,17]. Current posture categorization for risk rating
57 adjustments relies on ambiguous descriptors, such as "abducted" versus "not abducted" [5,6]. These
58 classifications often assume an ideal boundary of 0°, with no tolerance for natural variation when
59 determining adjustment factors. This rigid scoring method overlooks the practical realities faced by
60 construction workers, whose anatomical structure and natural postural sway make it impossible to
61 consistently maintain a 0° body joint angle [18,20]. As a result, ergonomic assessment outcomes are prone
62 to overestimation and fluctuation, particularly during continuous movements. Advanced motion detection
63 techniques, which measure joint angles with decimal-level precision, can exacerbate this issue.
64

65 In response to this limitation, this study proposes modifications to the REBA and RULA methods by
66 integrating sEMG signal analysis in postural sway experiments. The study is structured into two key phases:
67 (1) determining shoulder joint tolerance for the adjustment risk rating process through the analysis of muscle
68 activation patterns and (2) developing a revised ergonomic risk assessment framework that incorporates
69 joint tolerances into the adjustment risk rating process. The outcomes of this study are expected to mitigate
70 the overestimation issues inherent in REBA and RULA while introducing a novel integration of muscle status
71 and risk detection, thereby providing a more accurate and comprehensive approach to ergonomic
72 assessment.
73

74

75 **2. RELATED WORK**

76
77 This section provides a comprehensive review of ergonomic risk assessment approaches, tracing their
78 development from traditional methods to advanced technologies.
79

80 **2.1 Conventional approaches for ergonomic risk assessment**

81
82 Several rule-based observational assessment methods are widely used globally, including the OWAS [4],
83 RULA [5], and REBA [6]. OWAS evaluates risk levels across different body segments by assessing workers'
84 awkward postures in manufacturing environments. Whereas RULA specifically focuses on calculating joint
85 angles to determine risk scores for upper limb movements, REBA expands this approach by incorporating
86 full-body posture analysis into its assessment framework. These rule-based assessments fundamentally
87 depend on accurate posture descriptions as their primary input, rendering the precision of collected posture
88 data essential for the reliability of assessment results [7,21]. However, when joint angles approach category
89 boundaries, observers may struggle to distinguish between risk levels, leading to inconsistencies and intra-
90 /inter-observer reliability issues [22]. Additionally, rule-based observational methods are time-intensive and
91 costly due to the reliance on manual assessment [23]. Given these limitations, conventional approaches
92 require improvements to enhance their efficiency and accuracy.
93

94 **2.2 Advanced technologies for ergonomic risk assessment**

95
96 A wide range of advanced technologies has been utilized to detect risk factors associated with WMSDs for
97 construction workers. The following two main categories are mainly discussed: 1) approaches that enhance
98 the accuracy of joint angle measurements by leveraging MoCap system; 2) approaches that focus on
99 physiological data to assess risk at the biomechanical level.
100

101 The first type of approaches builds upon the fundamentals of rule-based ergonomic assessment methods
102 by providing more objective and accurate joint angle inputs while automating the evaluation process. These
103 implementations primarily utilize MoCap system to obtain precise joint coordinates. MoCap-based methods

104 include IMU and optical MoCap. IMUs are designed to measure acceleration, angular velocity, and, in
 105 certain instances, magnetic field strength. The compact, lightweight, and high-capacity nature of IMUs
 106 makes them particularly suitable for human activity recognition and the prevention of WMSD [24,25].
 107 Humadi et al. experimentally investigate the validity of RULA assessment using IMUs, reporting a minimum
 108 mean error of approximately 0.3° for upper-arm flexion among all measured joint angles [26]. However, the
 109 requisite skin-tight sensor attachment for noise reduction may restrict natural movements and impair work
 110 efficiency in construction settings. [27].

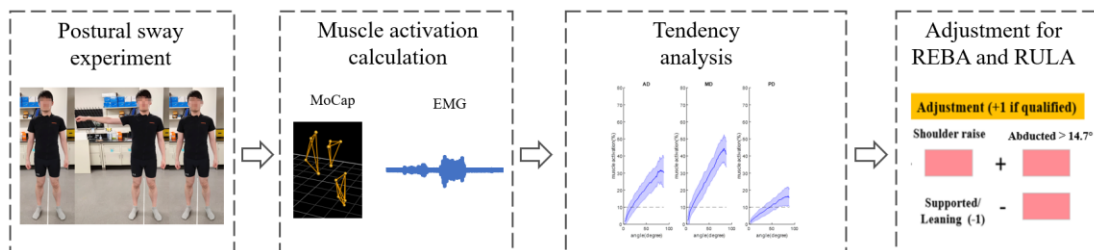
111
 112 The optical MoCap system represents an alternative approach for collecting highly accurate joint angle
 113 data. This system uses multiple calibrated cameras to track reflective markers on a subject, capturing their
 114 3D spatial and temporal coordinates from various angles for motion reconstruction [28]. As a result, the
 115 accuracy of such a system can reach millimeter-level precision [29]. However, optical MoCap systems are
 116 constrained by high costs, sensitivity to lighting conditions, and the need for a controlled environment, which
 117 limits their application in outdoor measurements for construction tasks [30].

118
 119 The second type of approaches relies on direct measurements using physiological sensors to monitor the
 120 physical status of the human body. For instance, sEMG is crucial for muscle activity analysis because it
 121 provides electrical activity of muscles during contraction and relaxation, offering valuable insights into
 122 muscle control function and the loads experienced by tissues and joints [31]. Although it cannot measure
 123 kinematics data, as a non-invasive method, sEMG signal can be used to predict muscle activity and muscle
 124 fatigue. A variety of signal analysis techniques are employed to extract meaningful fatigue-related
 125 information from raw EMG data. Amplitude-based metrics, such as root mean square (RMS) and mean
 126 absolute value (MAV), reflect a decline in force production as muscles fatigue. Similarly, frequency domain
 127 analyses, including power spectral density, capture shifts in the EMG spectrum toward lower frequencies
 128 during sustained or fatiguing contractions [15,32,33]. Ranavolo et al. determine the sEMG-based indices
 129 of 12 trunk muscles to evaluate the danger of lifting tasks [34]. Johns et al. examine the agreement between
 130 5 ergonomic risk assessment methods by recording sEMG during 4 sawmill tasks [35].

131
 132 Although these advanced MoCap-based methods provide accurate joint angles input for ergonomic risk
 133 assessment tools, the evaluated risk score will suffer from overestimation and fluctuation issues due to the
 134 intrinsic drawbacks of the adjustment risk rating process. To address this limitation, this study investigates
 135 the tolerance for adjustment factors by analyzing muscle activation during body segmental movement. A
 136 postural sway-incorporated ergonomic risk assessment method is then developed to alleviate the
 137 overestimation and fluctuation issues in the current REBA and RULA systems.

138
 139
 140 **3. METHODOLOGY**

141
 142 Workflow of this study is presented in Fig. 1. This methodology part will discuss data acquisition and
 143 experiment procedure.



144
 145
 146 Fig. 1: Workflow for developing postural sway-incorporated ergonomic risk assessment method.
 147

148 **3.1 Data acquisition**

149
 150 This study primarily focuses on the adjustment factors for the upper arm. Consequently, arm abduction was
 151 selected for investigation. These movements were performed at the Syncrude Centre at Glenrose

152 Rehabilitation Hospital and the Occupational Ergonomics Research Lab at the University of Alberta. In total,
 153 twenty-five right-handed subjects (15 male, 10 female) were recruited from the student population from the
 154 university. The subjects aged between 21 and 32 years, with body mass ranging from 52 to 86 kg and no
 155 history of injury to the relevant body parts. Prior to the experiments, the procedures and potential risks were
 156 explained, and informed consent was obtained. Ethics approval was granted by the University of Alberta
 157 (ethics approval: Pro00129961).

159 Three sEMG electrodes were placed on the right arm to record electrical muscle activity, representing
 160 muscle activation across the following muscles: the anterior deltoid (AD), middle deltoid (MD), and posterior
 161 deltoid (PD). Prior to the experiments, the areas of electrode attachment were cleaned with alcohol wipes
 162 to ensure proper skin preparation. The MA300 electromyography system (10 channels) and the Delsys
 163 Trigno Centro system (14 channels) were used to collect the sEMG data. The subject's movements were
 164 recorded by Vicon MoCap system. Ten reflective markers were attached to the subject's right arm and trunk
 165 to capture joint motion during the experiment. The marker trajectories were then used to calculate the joint
 166 angles of the upper arm. Fig. 2 shows the placement of sEMG sensors and markers.

168 In this article, the endurance limit is assigned as the tolerance for arm abduction. The endurance limit is
 169 defined as the threshold percentage of maximum voluntary contraction (%MVC) below which a posture or
 170 static muscular activity can be sustained for an indefinite period without resulting in muscle fatigue [36].
 171 Jørgensen et al. propose that the endurance limit for sustained contractions is approximately one hour at
 172 10% MVC [37]. This 10% MVC value is adopted in the present study to represent the tolerance for
 173 adjustment factors.

174

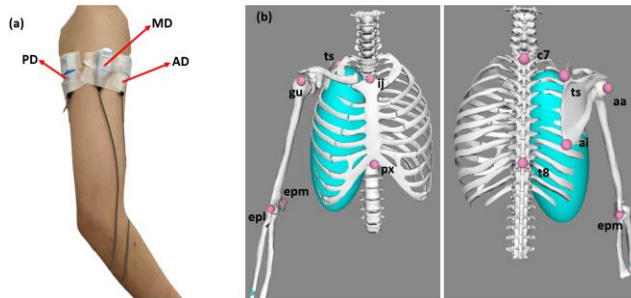


Fig. 2: (a) sEMG sensors placement; (b) markers placement.

175
 176
 177

3.2 Experiment procedure

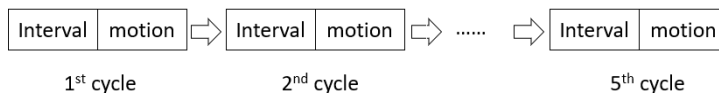
178

179 First, three different maximum voluntary contraction (MVC) tests were performed to normalize EMG data:
 180 1) AD: Subject flexes the shoulder to 90° with an extended elbow while resisting downward force applied
 181 to distal forearm. 2) MD: Subject abducts the shoulder to 90° in the frontal plane with an extended elbow,
 182 resisting downward force at the distal forearm. 3) PD: Subject positions the shoulder in 90° of abduction
 183 with slight horizontal abduction and resists forward-directed force on the distal forearm.

184

185 For the formal experiment, subjects were instructed to perform arm abduction. The subjects began with
 186 their right arm hanging naturally, palm facing medially, in preparation (natural posture). They then raised
 187 their right arm to a 90°, held this position for 5 seconds, and lowered it back down. The formal experiment
 188 included 5 cycles with 8-second intervals before each cycle. During the interval phase, the subjects are
 189 instructed to maintain a relaxed, neutral posture, allowing for the observation of changes in joint angles and
 190 muscle activation levels while participants remain relaxed. The joint angle and muscle activation gathered
 191 during this interval stage provide insights into baseline muscle activation and joint angle values before
 192 initiating motion. The complete experiment procedure is illustrated in Fig. 3.

193



195
 196

Fig. 3: Configuration of formal experiment.

197
198
199
200
201
202
203
204
205
206
207
208
209
210
211
212
213
214
215
216
217
218
219
220
221
222
223
224
225
226
227
228
229
230
231
232
233
234
235
236
237
238

3.3 Data processing

All sEMG data from the formal experiments and MVC tests were first baseline-corrected. The sEMG data were then full-wave rectified and digitally bandpass filtered (10–1000 Hz) using a second-order Butterworth filter [38]. The RMS was calculated using a 200-ms sliding window [39]. To minimize variability across channels, the amplitude of all sEMG data for each subject was normalized to the MVC value of the same muscle using the RMS amplitude measure.

For joint angle calculations, measurements were required in the sagittal, frontal, and horizontal planes. Each segment was treated as a two-ended joint and represented in vector form, shown in Eq. 1:

$$[1] V_{a-b} = J_a - J_b$$

$$[2] V_{a-b}^P = V_{a-b} \cdot \frac{P}{\|P\|^2}$$

$$[3] \theta_{ab,cd}^P = \arccos\left(\frac{V_{a-b}^P \cdot V_{c-d}^P}{\|V_{a-b}^P\| \cdot \|V_{c-d}^P\|}\right)$$

Where V_{a-b} represents the vector pointing from joint a (J_a) to joint b (J_b). The vectors were then projected onto the relevant planes (P), and the arc cos function was applied to compute joint angles ($\theta_{ab,cd}^P$) between the two projected vectors, shown in Eq. 2, Eq. 3. Further analyses were conducted to obtain muscle activation-joint angle curves. For each subject, an ensemble average of 5 cycles was calculated. Then, a grand ensemble average of subjects was assembled for each muscle.

4. RESULTS AND DISCUSSION

4.1 Experiment results

The RMS parameter represents the average intensity of the EMG signal, providing an overall measure of muscle activation. Therefore, muscle activation for each muscle is quantified using RMS, which is calculated over the entire motion window. The RMS results for arm abduction are presented in Fig. 4. The numbers in brackets indicate the number of subjects included for each specific muscle. A lower sample size for certain muscles results from EMG electrode displacement during the experiment or the muscle not being sufficiently active.

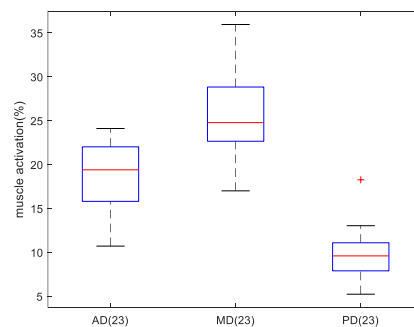
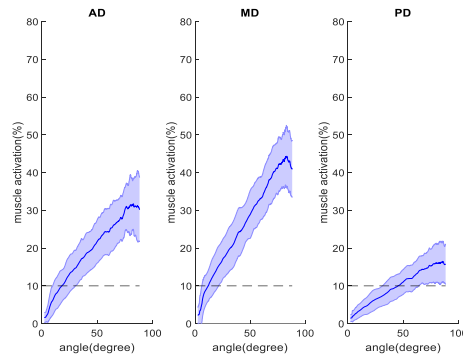


Fig. 4: Overall muscle activation in arm abduction.

For the average intensity of the EMG data, all selected muscles generally exhibit lower activation levels. During arm abduction, the highest average activation is observed in MD at 24.77% MVC. However, the PD showed an activation level of 9.59% MVC, which doesn't exceed the 10% MVC endurance limit. These results suggest that the muscles involved don't need to exert significant force during the arm abduction, as

239 participants perform the movements without additional weight and at a self-selected, comfortable speed.
240 These controlled conditions are designed to replicate the 0 Force/Load scenario in REBA and RULA.
241

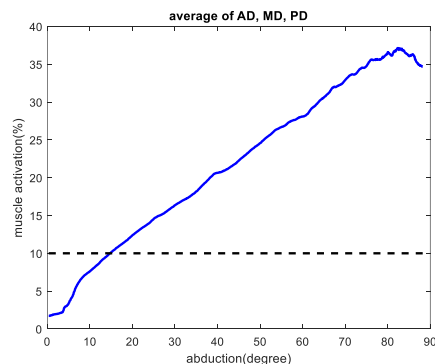
242 To visually analyze changes in muscle activation throughout the entire movement, the grand ensemble
243 averages of all participants are computed and examined for each muscle. These averages offer a
244 comprehensive perspective on muscle activation patterns across various joint and body segment
245 movements. Such findings contribute to research on joint boundaries and tolerance definitions in REBA
246 and RULA, as these scoring frameworks primarily rely on body posture assessments. Fig. 5 illustrates the
247 muscle activation–joint angle relationships for arm abduction, with grand ensemble averages and their
248 standard deviations displayed.
249



250
251
252 Fig. 5: Muscle activation–joint angle relationships for arm abduction.

253 There are several common trends observed across the three movements. Muscle activation consistently
254 increases as joint angles increase, with peak activation occurring before reaching the maximum joint angle,
255 followed by a subsequent decrease. Although the specific joint angle at which activation exceeds 10% of
256 MVC varies, all muscles eventually surpass this threshold. Additionally, the rate of increase in activation
257 (slope) remains relatively constant for each muscle during the rising phase of the curve. Some motion-
258 specific findings are also noted. In arm abduction, PD exhibits a more gradual increase in activation
259 compared to AD and MD, causing it to reach 10% of MVC later, around the midpoint of the movement.
260 Additionally, AD and MD display a steep rise in activation at the early stage of movement (joint angles less
261 than 10°), followed by a slower and steadier increase until reaching peak activation.
262

263 To determine the final angle tolerance for adjustment factors in REBA and RULA, the activation curves of
264 muscles are weighted and averaged to generate a generalized intensity pattern of muscle activation in
265 relation to joint angles. The result is illustrated in Fig. 6. For arm abduction, the contribution of the three
266 deltoid muscles varies. While no studies have explicitly quantified the percentage contribution of each
267 muscle, previous research suggests that MD generates significant abduction torque, accounting for up to
268 65% of the total torque [40]. Based on this finding, the weighting factors for the deltoid muscles are assigned
269 as follows: AD (17.5%), MD (65%), and PD (17.5%). The joint tolerance of arm abduction is 14.7°.
270



271

Fig. 6: Generalized muscle activation in relation to joint angle.

Natural postural sway is observed during the 8-second neutral posture phase, which is required before each subject engages in the formal motions. Table 1 shows the average joint angle values and muscle activation for each subject during this neutral posture phase.

Table 1: Average joint angle and muscle activation during neutral posture phase.

Motion	Average joint angle (degree)	Average AD activation (%)	Average MD activation (%)	Average PD activation (%)
Arm abduction	1.62	2.22	2.32	1.46

4.2 Discussion

For the interval stage, the average joint angle measurements reveal that body joints exhibit subtle movements during natural posture. While these movements are typically less than 2°, which are not easily perceptible to the human eye. However, they can be precisely captured through the use of advanced measurement devices. Given that workers' joint angles naturally fluctuate within a small range rather than remaining precisely at 0°, a physiologically impossible posture, even minor changes in joint angles result in corresponding variations in adjustment factor values. Thus, this introduces significant variability in the final results of REBA and RULA, contributing to severe fluctuation issues in the assessment outcomes. Furthermore, the average muscle activation results indicate that the relevant muscles are activated at a low level prior to the commencement of formal motion. Specifically, the activation of all muscles was below 3%, which remains less than half of the endurance limit. As a result, workers are unlikely to experience any risk under these conditions. However, this pre-activation contributes to an overestimation issue in the final assessments of REBA and RULA. For arm abduction, the tolerance is 14.72°, approximately 16.36% of the entire motion. Therefore, the potential risk, as indicated by muscle activation, emerges as early as around 16% of the total movement, rather than at the outset. Consequently, this also indicates existing REBA and RULA adjustment rating systems are inadequate and require revision.

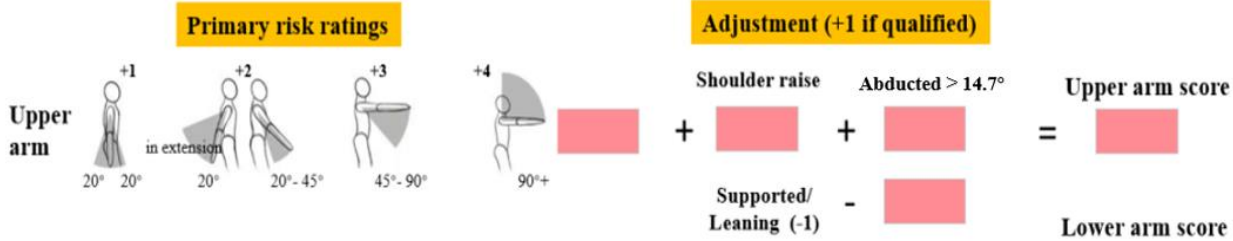
By examining the average activation-angle curve results, several common patterns can be identified that are relevant to the new adjustment rating process. The curves exhibit a similar shape: muscle activation increases from the start, reaching a peak value before the peak joint angle, and then decreases. To understand the behavior of these curves, two parameters—slope and peak activation value—are analyzed. The slope represents the rate of change in muscle activation. Before the peak activation point, the curves always show an upward trend, with a steeper curve indicating a rapid increase in activation, which could signal potential danger. For arm abduction, the curve slope is relatively gentle at the beginning of the movement but becomes steeper between 4° and 9°. After this point, the slope remains moderate until reaching the peak activation. Although there is a noticeable slope change during the early phase, it is important to note that the activation level during this phase remains below 10%, indicating a safe range for workers. Therefore, a detailed categorization of risk based on slope change is unnecessary for arm abduction.

While the MVC% value does not directly reflect the degree of danger for workers, it serves as an indicator of muscle activation intensity. High MVC% movements can lead to more rapid muscle fatigue. Sustained high-intensity contractions deplete energy reserves and accumulate metabolic by-products, contributing to fatigue [41]. The peak activation value represents the maximum intensity of the movement and can be used to assess the potential for muscle fatigue. The average muscle curves show a peak activation value below 40%, which is considered indicative of low-intensity tasks. Consequently, establishing a detailed risk classification based on the peak activation value is not necessary. Considering that this study focuses on adjustment factors, a simpler binary rule (+1 for any abduction) is sufficient for evaluating potential risks.

4.3 Revised REBA and RULA

Due to the presence of postural sway, the adjustment factor risk score definitions in the original REBA and RULA models suffer from overestimation and fluctuation issues, as they overlook minor joint movements.

324 Based on endurance limit values, this study determines shoulder joint angle tolerance by focusing on the
 325 muscle activation performance of muscles associated with arm abduction. The consistent slope and lower
 326 peak activation values indicate that a binary rule based on joint angle tolerance is sufficient to assess
 327 potential risks when calculating the adjustment factor. The revised REBA method (upper arm adjustment
 328 factor) is illustrated in Fig 7.
 329



330
 331 Fig 7: Revised REBA method (upper arm adjustment factor)
 332

333 **4.4 Limitation**

334 Although the postural sway-integrated REBA and RULA address overestimation and fluctuation issues,
 335 several limitations have still been identified. 1) Limitations in the choice of subjects and tasks. Expanding
 336 the sample size is crucial to further investigate the potential relationships between mobility, gender, and
 337 age. In addition, future studies will involve construction workers as participants to collect data reflective of
 338 real-world practices. Joint tolerances also should be evaluated across different types of construction tasks
 339 to determine whether task-specific differences require adjustments to joint tolerances. 2) Limitations in the
 340 number of selected muscles. Three muscles were selected for arm abduction to represent muscle activation
 341 intensity through changes in MVC%. However, these muscles may not fully represent the corresponding
 342 motion. Future work could involve conducting detailed experiments that measure the muscle activity of
 343 additional muscles involved in these movements. 3) Limitations in joint angle categories. The experiments
 344 primarily focus on adjustment factors related to the upper arm due to the limited time. However, REBA and
 345 RULA also include adjustment factors for the neck and trunk. To develop a comprehensive risk assessment
 346 method, future research should investigate the remaining adjustment factors and establish primary score
 347 boundaries for the arm, wrist, neck, and trunk.
 348

349
 350 **5. CONCLUSIONS AND FUTURE DIRECTION**

351 This study primarily contributes to the field of occupational health and safety management for construction
 352 workers by developing revised ergonomic risk assessment methods based on the current REBA and RULA
 353 systems. These revised methods provide a more accurate evaluation of potential risks associated with
 354 construction tasks. It addresses the inherent limitations of existing assessment methods, which are often
 355 characterized by overestimation and fluctuation due to rigid adjustment factor boundaries that fail to account
 356 for joint tolerances and overlook natural postural sway. To overcome these limitations, this study analyzes
 357 the activation levels of relevant muscles to determine the joint angles corresponding to the endurance limit,
 358 which are then used as the tolerance for adjustment factors. The methodology consists of two main steps:
 359 (1) identifying joint tolerances based on muscle activation changes from arm abduction experiments, and
 360 (2) developing the revised postural sway-integrated REBA and RULA methods.
 361

362 The joint angle and muscle activation results during the interval stage highlight the common occurrence of
 363 postural sway in the shoulder, which contributes to overestimation and fluctuation issues in traditional REBA
 364 and RULA methods. By assessing the joint angle corresponding to the endurance limit, this study provides
 365 a biomedical perspective to enhance ergonomic risk assessments. Although the postural sway-integrated
 366 REBA and RULA address overestimation and fluctuation issues by accounting for minor joint movements
 367 in comparison to the traditional REBA and RULA methods, several limitations have still been identified. 1)
 368 Limitations in the number of subjects: A total of 25 subjects participated in this experiment. However, due
 369 to challenges with EMG sensor attachment and motion capture data processing, data from fewer than 25
 370 subjects were ultimately available. Consequently, expanding the sample size is crucial to further investigate
 371

372 the potential relationships between mobility, gender, and age. 2) Limitation in MoCap data errors. Inherent
373 errors arise in the gap-filling process, as it relies on estimates derived from the quality of the surrounding
374 data. Moving forward, a more comprehensive ergonomic risk assessment model that incorporates postural
375 sway should be developed. This model will also address limitations related to the number of subjects and
376 MoCap data errors by expanding the participant pool and utilizing additional motion capture cameras to
377 enhance data accuracy.

378
379
380
381

REFERENCES

- 382 [1] Gagnon, G., Sekkay, F., Imbeau, D., & Bourgault, M. 2024. Analyzing Occupational Accidents and
383 Exoskeleton Potential in the Construction Industry in Québec, Canada. *IISE Transactions on
384 Occupational Ergonomics and Human Factors*, 1–19.
- 385 [2] [https://www.canada.ca/en/employment-social-development/services/health-safety/reports/2022-
386 injuries.html](https://www.canada.ca/en/employment-social-development/services/health-safety/reports/2022-injuries.html)
- 387 [3] Cheng, C. W., Leu, S. Sen, Lin, C. C., & Fan, C. 2010. Characteristic analysis of occupational
388 accidents at small construction enterprises. *Safety science*, 48(6), 698–707.
- 389 [4] Karhu, O., P. Kansil, and I. Kuorinka. 1977. Correcting working postures in industry: A practical
390 method for analysis. *Appl. Ergon.* 8 (4): 199–201.
- 391 [5] McAtamney, L., and E. Nigel Corlett. 1993. RULA: A survey method for the investigation of work-
392 related upper limb disorders. *Appl. Ergon.* 24 (2): 91–99.
- 393 [6] Hignett, S., and L. McAtamney. 2000. Rapid entire body assessment (REBA). *Appl. Ergon.* 31 (2):
394 201–205.
- 395 [7] Ryu, JuHyeong, et al. 2021. Analysis of the limits of automated rule-based ergonomic assessment
396 in bricklaying. *Journal of Construction Engineering and Management* 147.2: 04020163.
- 397 [8] David, Geoffrey C. 2005. Ergonomic methods for assessing exposure to risk factors for work-
398 related musculoskeletal disorders. *Occupational medicine* 55.3: 190-199.
- 399 [9] Wang, Di, Fei Dai, and Xiaopeng Ning. 2015. Risk assessment of work-related musculoskeletal
400 disorders in construction: State-of-the-art review. *Journal of Construction Engineering and
401 management* 141.6: 04015008.
- 402 [10] Vignais, Nicolas, et al. 2017. Physical risk factors identification based on body sensor network
403 combined to videotaping. *Applied ergonomics* 65: 410-417.
- 404 [11] Vena, Alessandro, et al. 2011. Three-dimensional kinematic analysis of the golf swing using
405 instantaneous screw axis theory, part 1: Methodology and verification. *Sports Engineering* 13: 105-
406 123.
- 407 [12] Zhao, J., and E. Obonyo. 2021. Applying incremental deep neural networks-based posture
408 recognition model for ergonomics risk assessment in construction. *Adv. Eng. Inf.* 50 (Oct): 101374.
- 409 [13] Lee, Yu-Chi, et al. 2022. SEE: a proactive strategy-centric and deep learning-based ergonomic risk
410 assessment system for risky posture recognition. *Advanced Engineering Informatics* 53: 101717.
- 411 [14] Mudiyansele, Srimalatha E., et al. 2021. Automated workers' ergonomic risk assessment in
412 manual material handling using sEMG wearable sensors and machine learning. *Electronics* 10.20:
413 2558.
- 414 [15] Li, X., Komeili, A., et al. 2017. A framework for evaluating muscle activity during repetitive manual
415 material handling in construction manufacturing. *Automation in Construction*, 79, 39-48.
- 416 [16] Kee, Dohyung. 2021. Comparison of OWAS, RULA and REBA for assessing potential work-related
417 musculoskeletal disorders. *International Journal of Industrial Ergonomics* 83: 103140.
- 418 [17] Kee, Dohyung, Seokhee Na, and Min K. Chung. 2020. Comparison of the Ovako working posture
419 analysis system, rapid upper limb assessment, and rapid entire body assessment based on the
420 maximum holding times. *International Journal of Industrial Ergonomics* 77: 102943.
- 421 [18] Kim, Jiwon, et al. 2012. Relationship between body factors and postural sway during natural
422 standing. *International Journal of Precision Engineering and Manufacturing* 13: 963-968.
- 423 [19] Day, B. L., et al. 1993. Effect of vision and stance width on human body motion when standing:
424 implications for afferent control of lateral sway. *The Journal of physiology* 469.1: 479-499.
- 425 [20] Danna-Dos-Santos, Alexander, et al. 2008. Is voluntary control of natural postural sway possible?
426 *Journal of motor behavior* 40.3: 179-185.

- 427 [21] Andrews, D. M., A. M. Holmes, P. L. Weir, T. A. Arnold, and J. P. Callaghan. 2008. Decision times
428 and errors increase when classifying trunk postures near posture bin boundaries. *Theor. Issues*
429 *Ergon. Sci.* 9 (5): 425–440.
- 430 [22] Plantard, P., H. P. Shum, A.-S. Le Pierres, and F. Multon. 2017. Validation of an ergonomic
431 assessment method using Kinect data in real workplace conditions. *Appl. Ergon.* 65 (Nov): 562–
432 569.
- 433 [23] Ghasemi, Fakhradin, and Neda Mahdavi. 2020. A new scoring system for the Rapid Entire Body
434 Assessment (REBA) based on fuzzy sets and Bayesian networks. *International Journal of Industrial*
435 *Ergonomics* 80: 103058.
- 436 [24] Antwi-Afari, M. F., Y. Qarout, R. Herzallah, S. Anwer, W. Umer, Y. Zhang, and P. Manu. 2022.
437 Deep learning-based networks for automated recognition and classification of awkward working
438 postures in construction using wearable insole sensor data. *Autom. Constr.* 136 (Apr): 104181.
- 439 [25] Zhang, H., X. Yan, and H. Li. 2018. Ergonomic posture recognition using 3D view-invariant features
440 from single ordinary camera. *Autom. Constr.* 94 (Oct): 1–10.
- 441 [26] Humadi, Ahmed, et al. 2021. In-field instrumented ergonomic risk assessment: Inertial
442 measurement units versus Kinect V2. *International Journal of Industrial Ergonomics* 84: 103147.
- 443 [27] Valero, Enrique, et al. 2016. Musculoskeletal disorders in construction: A review and a novel
444 system for activity tracking with body area network. *Applied ergonomics* 54 (2016): 120-130.
- 445 [28] Guess, Trent M., et al. 2022. Comparison of Azure Kinect overground gait spatiotemporal
446 parameters to marker based optical motion capture. *Gait & posture* 96 (2022): 130-136.
- 447 [29] Merriault, Pierre, et al. 2017. A study of vicon system positioning performance. *Sensors* 17.7
448 (2017): 1591.
- 449 [30] Aminian K, Najafi B. 2004. Capturing human motion using body - fixed sensors: outdoor
450 measurement and clinical applications. *Computer animation and virtual worlds*, 15(2): 79-94.
- 451 [31] Lindstrom, L., R. O. L. A. N. D. Kadefors, and I. N. G. E. M. A. R. Petersen. 1977. An
452 electromyographic index for localized muscle fatigue. *Journal of applied physiology* 43.4 (1977):
453 750-754.
- 454 [32] Gautam, Yogesh, and Houtan Jebelli. 2024. Design of flexible polyimide-based serpentine EMG
455 sensor for AI-enabled fatigue detection in construction. *Sensing and Bio-Sensing Research* 46
456 (2024): 100713.
- 457 [33] Jebelli, Houtan, and SangHyun Lee. 2019. Feasibility of wearable electromyography (EMG) to
458 assess construction workers' muscle fatigue. *Advances in Informatics and Computing in Civil and*
459 *Construction Engineering: Proceedings of the 35th CIB W78 2018 Conference: IT in D61 esign,*
460 *Construction, and Management.* Springer International Publishing, 2019.
- 461 [34] Ranavolo, Alberto, et al. 2018. Surface electromyography for risk assessment in work activities
462 designed using the “revised NIOSH lifting equation”. *International Journal of Industrial Ergonomics*
463 68 (2018): 34-45.
- 464 [35] Jones, Troy, and Shrawan Kumar. 2010. Comparison of ergonomic risk assessment output in four
465 sawmill jobs. *International Journal of Occupational safety and ergonomics* 16.1 (2010): 105-111.
- 466 [36] Imbeau, Daniel, and Bruno Farbos. 2006. Percentile values for determining maximum endurance
467 times for static muscular work. *International journal of industrial ergonomics* 36.2: 99-108.
- 468 [37] Jørgensen, Kurt, et al. 1988. Electromyography and fatigue during prolonged, low-level static
469 contractions. *European journal of applied physiology and occupational physiology* 57: 316-321.
- 470 [38] Georgakis, Apostolos, et al. 2003. Fatigue analysis of the surface EMG signal in isometric constant
471 force contractions using the averaged instantaneous frequency. *IEEE transactions on biomedical*
472 *engineering* 50.2: 262-265.
- 473 [39] Asogbon, Mojisola Grace, et al. 2018. Effect of window conditioning parameters on the
474 classification performance and stability of EMG-based feature extraction methods. *2018 IEEE*
475 *International Conference on Cyborg and Bionic Systems (CBS).* IEEE.
- 476 [40] Escamilla, Rafael F., et al. 2009. Shoulder muscle activity and function in common shoulder
477 rehabilitation exercises. *Sports medicine* 39: 663-685.
- 478 [41] Enoka, Roger M., and Jacques Duchateau. 2008. Muscle fatigue: what, why and how it influences
479 muscle function. *The Journal of physiology* 586.1: 11-23.
- 480
481